

Calibrated Out-of-Distribution Detection with a Generic Representation

Tomáš Vojtík^{*†}, Jan Šochman[†], Rahaf Aljundi[‡], and Jiří Matas[†]

[†]CMP Visual Recognition Group, FEE, Czech Technical University in Prague

[‡]Toyota Motor Europe, Brussels, Belgium

Abstract

Out-of-distribution detection is a common issue in deploying vision models in practice and solving it is an essential building block in safety critical applications. Existing OOD detection solutions focus on improving the OOD robustness of a classification model trained exclusively on in-distribution (ID) data. In this work, we take a different approach and propose to leverage generic pre-trained representations. We first investigate the behaviour of simple classifiers built on top of such representations and show striking performance gains compared to the ID trained representations. We propose a novel OOD method, called GROOM, that achieves excellent performance, predicated by the use of a good generic representation. Only a trivial training process is required for adapting GROOM to a particular problem. The method is simple, general, efficient, calibrated and with only a few hyper-parameters. The method achieves state-of-the-art performance on a number of OOD benchmarks, reaching near perfect performance on several of them. The source code is available at <https://github.com/vojirtom/GROOM>.

1. Introduction

The problem of detection of out-of-distribution data points, OOD in short, is important in many computer vision applications [1, 19, 4]. One can even argue that no model obtained by machine learning on a training set \mathcal{T} should be deployed without the OOD ability, since in practice it is almost never the case that all the data the model will make predictions on will be drawn from the same distribution that generated \mathcal{T} [49]. For undetected out-of-distribution data, the prediction will in general be arbitrary, with possibly grave real-world consequences, especially in safety-critical applications. The importance and ubiquity of OOD is evidenced by the fact that virtually the same problem has

emerged in different contexts under different names - open set recognition, anomaly or outlier detection, and one-class classification.

The reasons for test data not being from the training set distribution are diverse; they often influence the terminology used. In open set recognition (OSR) [24, 46], the semantic shift is considered, i.e. the introduction of new classes at test time. Failures of the measurements system generate outlier data. In anomaly detection, the presence of out-of-distribution data is assumed rare. A domain shift, e.g. when a classifier trained on real-world images is applied to clip art, leads to a severe data distribution change.

So far, prior art has mainly developed OOD detection models by supervised training on in-distribution (ID) data [46, 3, 2]. We follow the recent success of self-supervised representation model training and we are the first to investigate and apply it to out-of-distribution detection. This novel approach significantly improves OOD performance; experiments confirm the superiority of the generic representation over problem-specific approaches that train or fine-tune the feature extractor on a particular in-distribution (ID) training set.

Any good representation should enable solving a given, a priori unknown, downstream task. A good *generic* representation should enable solving multiple tasks without the need of fine-tuning on the task data. To verify the goodness and generality of tested representations, we first propose to use two simple classifiers: (i) linear probe (LP), and (ii) the nearest mean (NM) classifier which represents in-distribution classes by their mean. This already outperforms the state-of-the-art on a broad range of problems, often by a large margin. In fact, for many benchmarks, perfect or near perfect performance ($>99\%$) was reached.

This approach does not require any information about the out-of-distribution data, e.g. in the form of a few examples of the anomalies or outliers, and is thus applicable to all the standard setting of the OOD and OSR problems [46].

Since the LP and NM methods perform each well on different classes of the OOD problems, we formulate a

^{*}Corresponding author, vojirtom@fel.cvut.cz

Neyman-Pearson task [32, 27, 28] on their combination. We call this approach GROOM (for Generic Representation based OOD detection). It models the in-distribution as a 2D Gaussian in the space of LP and NM responses, and provides a robust solution to the OOD problem. To summarize, the contributions of the paper are:

- We show that using a generic pre-trained representation together with a simple classifier achieves state-of-the-art performance on a number of OOD benchmarks.
- We formulate the OOD detection as a Neyman-Pearson task in the space of LP and NM scores. The operating point is selected by the allowed false negative rate for *all* in-classes. This results in a well calibrated classification score on the ID task.
- The proposed method outperforms the state-of-the-art by a large margin on most of OOD problems and even saturates several commonly used benchmarks.

2. Related Work

Out-of-distribution (OOD) detection refers to the identification of test samples that are drawn from a different distribution than the underlying training distribution of a given classification model. Hendrycks et al. [12] was one of the first to explore this problem with modern neural networks using maximum softmax probability (MSP) obtained from a classification model as a detection score. While being a classical baseline in OOD detection, MSP can output high ID probabilities for unknown OOD samples [33]. Subsequent work has attempted to provide more robust OOD detection by either operating on a fixed model, or performing additional ID training or even leveraging auxiliary OOD data. We refer to [46] for a complete survey on the different lines of OOD detection research.

Post-hoc methods usually define different OOD detection scores or perform manipulation of the input samples to increase the separability between the distributions of ID and OOD scores [22, 16]. As a more robust alternative to the MSP scores, [23] proposed to use the energy of the output logits as a scoring function showing strong improvements over MSP and more separable scores. Recently, [10] showed that using maximum logit as an OOD detection score is significantly more robust than MSP, suggesting that the normalization of the probability by the closed set classes is the source for the overconfident predictions.

Of the distance based detection scores, we mention [21] which estimates the Mahalanobis distance to the closest class. Based on the estimated L_2 distances in the learned embedding space, [34] propose instead to use the K-nearest neighbour (KNN) distance as detection score. KNN [34] improves significantly over the Mahalanobis distance [21].

Manipulating the logits of a pre-trained ID classifier has its limits, which led to the second group of approaches.

Training based methods target a stronger OOD detection performance through regularizing the training such that the resulting classifier or representations behave differently for ID compared to OOD inputs. Tackling the same overconfident issue as in post-hoc methods, [42] proposed to train the ID classification model while enforcing a constant logit norm. Deep ensemble [20] combines adversarial training with neural networks ensemble in addition to using the loss function as a scoring rule. The computational cost of such approach might be prohibitive for big networks.

Other work aims at regularizing the training with virtual representatives of OOD input. CSI [35] utilizes contrastive training and apply strong augmentations to the input images as an alternative to OOD data. Adversarial Reciprocal Points Learning (ARPL) [5] proposes the concept of "reciprocal" points as a proxy for OOD samples which are obtained by combined discriminative and metric learning. This method showed state-of-the-art OOD detection performance, however, it requires complex training scheme and large hyper-parameter tuning. The proposed method is significantly more efficient and improve over ARPL with a large margin in multiple benchmarks.

"A closed set classifier is all you need" [40] is a recent work suggesting that an improved training scheme that leads to better performance on ID data discrimination offers very competitive OOD detection quality that rivals that of OOD regularized training such as ARPL [5]. More recently, [45] has evaluated a wide range of OOD detection methods and their empirical results suggest that strong input augmentation techniques, e.g. MixUp [36], CutMix [47] and PixMix [15] are the most effective type of training methods for OOD detection.

The observations of [40] and [45] suggest that obtaining a more robust *closed ID* classification model either by sophisticated training techniques or strong input processing is a key to robust OOD detection. In this work we show that what matters the most is *not* the classification model trained specifically for ID data but rather a strong underlying feature extractor. We show that a generic representation such as CLIP [31] can serve as a basis for an extremely powerful OOD detector on a wide variety of benchmarks.

Pretrained representations have been shown to significantly boost the classification performance in the context of few shot learning [37] and continual learning [29], but are very rarely explored in the OOD detection literature. Hendrycks et al. [14] investigate the role of self-supervised pre-training on the *ID task data only*. In [13] Hendrycks et al., ImageNet pre-trained models are deployed. However, the pre-training was only leveraged as an initialization where the model is later finetuned on the specific ID task before the OOD detection is conducted.

We are the first, to the best of our knowledge, to show that generic, self-supervised trained representation can be directly leveraged for OOD detection on various ID tasks without any finetuning of the representation on those tasks. In other words, we suggest that one does not need to learn and capture the specificity of a given ID task (as opposed to e.g. [40]) but rather only a good metric space where similar (even out-of-distribution) samples lie nearby is sufficient.

3. The GROOD Method

In this section we describe the proposed Generic Representation based OOD detection approach, GROOD in short, which exploits a representation pre-trained on auxiliary large-scale non-OOD-related data. The intuition behind the method is that a generic representation is a good starting point for the OOD detection. The method also produces well-calibrated classification scores for a given ID task corresponding directly to the same false negative rate for every ID class.

We expect the representation to be strong, allowing in- and out-class data separation by a low-complexity classifier. In particular, we investigate two such classifiers, Linear Probe (LP) and Nearest Mean (NM), trained on ID data only. The LP classifier consists of a single linear projection layer followed by a softmax normalization (*i.e.* multi-class logistic regression model). This type of classifier has been used in representation learning to test the expressiveness of a representation [6]. The NM classifier assigns data to the class with the nearest class mean as measured by the L_2 distance; learning this classifier consists of computation of mean vector representation for each class. We chose the LP and NM classifiers because of (i) their simplicity – simple classifiers generalize well, do not overfit to ID problem – and (ii) complementarity – one is based on a discriminative score and the other on a distance metric – as illustrated in Fig 1. At the test time, when OOD data points are detected, the LP and MN classifier responses are simply thresholded (like in [40]) and this threshold is varied to compute the ROC curves in the experiments.

We show in Sec 4 that already with this setup one is already able to achieve state-of-the-art OOD results. Although each of these classifiers performs already better than state-of-the-art methods on most benchmarks, we show in Sec 4.5 that they are in fact complementary, each working better on different type of problems. Further, as shown in Sec 2, their logit/distance scores are not well calibrated, *i.e.* when setting an in-out decision threshold, the ID classes are rejected unevenly, some producing higher false negative rates than the others.

To solve these issues, we propose a new method, called GROOD, which combines the outputs of the two classifiers. The distribution of the outputs is modelled as a bi-variate Gaussian which permits addressing OOD as a formally de-

fined two-class Neyman-Pearson task [32, 27, 28] through which calibration of the OOD detector is achieved.¹

We illustrate the approach on an example OOD problem shown in Fig 3. CIFAR10 is considered ID (class 9 shown here) and the TinyImageNet represents an OOD dataset (see Sec 4 for details on datasets). The figure shows in green the ID and in red the OOD distribution of LP scores (top) and NM similarity (right), see Sec 4.3 for the definitions. The data are plotted as green (ID) and red (OOD) dots. The ID distribution is specified by the desired ID classification problem, the OOD distribution may vary depending on particular ID/OOD benchmark. Notice, that shifting the problem from a one-dimensional score (either LP or NM) to a two-dimensional space allows us to leverage the best of LP and NM (cf Fig 1) and leads to a better ID/OOD separation when considering jointly *all* tested OOD problems.

In the proposed GROOD method we model the ID distribution as a Normal distribution. Although an approximation, we observed empirically that it holds reasonably well over a wide range of tasks². Of course, nothing prevents us from using a more complex model of the distribution, *e.g.* the non-parametric Parzen estimate, if needed, but the Normal distribution assumption makes the next step in designing GROOD significantly easier. Next we formulate the ID/OOD classification problem as a multi-class Neyman-Pearson task [32, 27, 28]. We start by considering a single ID class. Let \mathcal{I} be a class representing the ID samples and \mathcal{O} the class for OOD data. Assume the data are sampled from a two-dimension domain $\mathcal{X} = \mathcal{X}_{LP} \times \mathcal{X}_{NM}$, where \mathcal{X}_{LP} is the domain of LP logit scores and \mathcal{X}_{NM} the domain of NM distances. The task is then to find a strategy $q^*(x) : \mathcal{X} \rightarrow \{\mathcal{I}, \mathcal{O}\}$ such that

$$\begin{aligned} q^* &= \arg \min_q \int_{x: q(x) \neq \mathcal{O}} p(x|\mathcal{O}) dx \\ \text{s.t. } \epsilon_{\mathcal{I}} &= \int_{x: q(x) \neq \mathcal{I}} p(x|\mathcal{I}) dx \leq \epsilon \end{aligned} \quad (1)$$

This optimization problem minimises the false ID acceptance rate for a particular ID class and bounds the maximal ID rejection rate by ϵ . For K classes we specify K such problems and use the same constant ϵ for all of them, so that the same fixed rejection rate is required for all classes.

It is known ([32]) that the optimal strategy for a given $x \in \mathcal{X}$ is constructed using a the likelihood ratio $r(x) = p(x|\mathcal{I})/p(x|\mathcal{O})$ so that $q(x) = \mathcal{I}$ if $r(x) > \mu$ and $q(x) = \mathcal{O}$ if $r(x) \leq \mu$. The optimal strategy q^* is obtained by selecting the minimal threshold μ such that $\epsilon_{\mathcal{I}} \leq \epsilon$. The problem

¹We experiment with 2D space of scores only, as the amount of data for model estimation is limited (100 or less examples in some cases).

²A breaking point would be the case of ID data where one class consists of multiple clusters. In this case, the NM classifier would need to be modified to consider several "means".

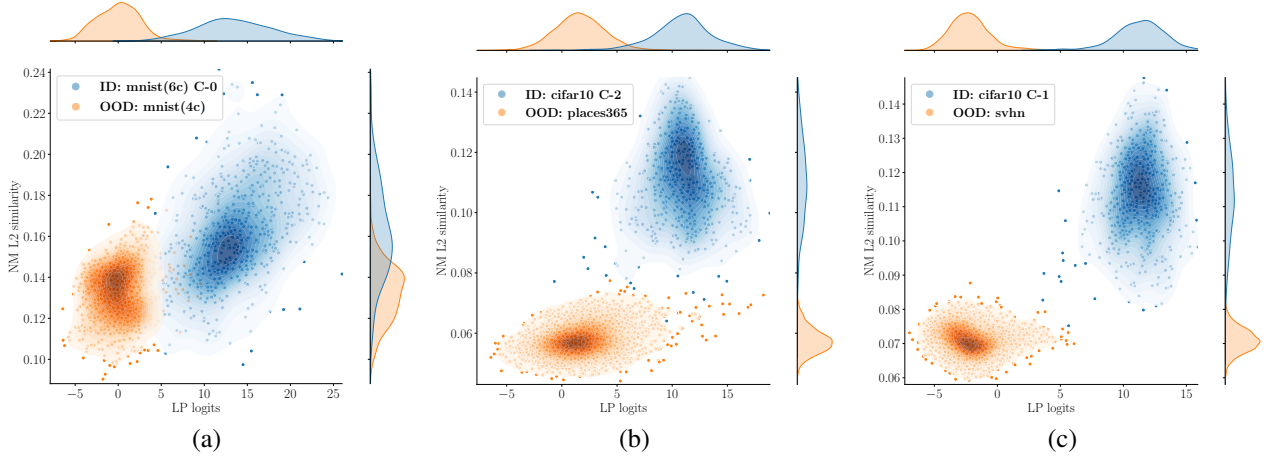


Figure 1. Complementarity of the LP and NM classifiers. (a) When applied to a problem with semantic shift only, the LP classifier tends to separate the ID and OOD datasets better. (b) For OOD problems with mixed semantic and domain shifts, NM classifier performs typically better. (c) On some problems, both perform well. Notice that moving from a single LP or NM similarity to a two-dimensional space already allows better separation in *all* cases. Compare this with detailed results in Tabs 2-5.

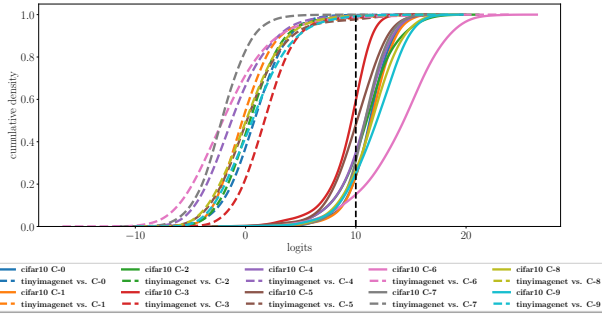


Figure 2. Mis-calibration of the logit scores. The graph shows cumulative distributions for ID (full line) and OOD (dashed) classes given the LP logit scores trained on the ID data. Here CIFAR10 is ID and TinyImageNet is OOD. Selecting a single logit threshold, 10 in this case, results in different ID class rejection rates. We call this *logits mis-calibration*.

is solved either analytically for some simple distributions (such as Gaussian) or numerically otherwise.

To solve this problem we still have to specify the $p(x|\mathcal{O})$ distribution. If we assume this distribution to be uniform in \mathcal{X} , we would decide based on the quantiles of the Normal distribution $p(x|I)$. However, we constructed \mathcal{X} not from general 1D random variables, but from the classification scores of LP and NM. It is thus reasonable to assume that the OOD data will lie in the region where the LP score and NM similarity are low.

To implement this assumption, we construct $p(x|\mathcal{O})$ as another Normal distribution with a zero mean and a diagonal covariance matrix with large variances. For the LP, the zero mean assumption is motivated by the fact that in high dimensional spaces, a random vector is likely to be close to orthogonal to the id-class directional vectors (the weights

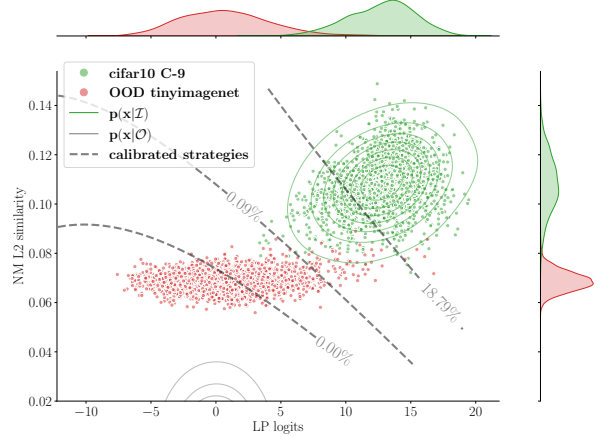


Figure 3. GROOD motivation diagram. Class 9 from CIFAR10 taken as ID and the TinyImageNet dataset as OOD. Two classifiers, LP and NM, produce a 2D space to which each sample is mapped to (green or red dots for ID and OOD respectively). Top/right axes: the marginal empirical distributions. The ID data are modelled as a bi-variate Normal distribution (green iso-lines). A "general" OOD distribution is constructed as another Normal distribution (gray iso-lines). Three possible decision strategies for different expected ID false rejection rates in the N-P task are plotted in black dashed lines with corresponding rejection rates marked. Note: The proposed methods do not have access to the OOD data, they are shown only to strengthen reader's intuition.

of the linear layer before the softmax). For the MN similarity, the choice was made empirically as a limit case for very large L2 distance from a class mean center. The variance, in both directions, is set so that the range of the data is a multiple of the in-distribution range, i.e. it is very broad. The in-distribution range was robustly estimated as a 90% quantile of all in-distribution data scores and the multiplicative

factor was set empirically. Both Normal distributions for ID and OOD are plotted in Fig 3 in green and gray solid line contours respectively. Fig 3 shows also three optimal strategies (if the assumptions about normality were true) and their corresponding ID rejection rates as gray dashed decision boundaries. Clearly, the strategy rejects the least confident ID samples first.

Solving this Neyman-Pearson problem for each ID class gives K strategies q_k^* , each calibrated for the same rejection rate. In practice, we would specify acceptable rejection rate ϵ and obtain the optimal strategies for normally distributed data. For the evaluation where we need to sweep over the values of ϵ , we sample a limited set of values, find their likelihood ratio μ and interpolate in-between.

Finally, for the ID classification we use the $\arg \max_k p_k(x|\mathcal{I})$ of the probabilities obtained as bivariate Normal distributions for each class k .

4. Experiments

In this section we evaluate the proposed GROOM method and other state-of-the-art methods on a wide and diverse set of benchmark problems described in the OOD literature. We select the benchmarks to cover various scenarios and to demonstrate the generality of the proposed approach.

4.1. Benchmarks

There are several commonly used benchmarks to evaluate OOD and OSR methods and most papers typically evaluate on their subset. In our evaluation we attempt to cover most of the commonly used variations. We categorize the experiments based on the presence/absence of the domain shift (DS) and the semantic shift (SS).

No DS, only SS. For MNIST [8], SVHN [26] and CIFAR10 [18] datasets we perform the 6-vs-4 split [5, 45, 40]. Here six classes are selected as ID at random and the remaining four as OOD. The experiment is repeated five times with different splits and the average metrics are reported together with their standard deviations.

For a bit larger CIFAR+10 and CIFAR+50 experiments, four classes are sampled from CIFAR10 and are considered ID and another 10 (or 50) non-overlapping classes are randomly selected from CIFAR100 [18] and used as OOD [5, 45, 40]. Again, five trials are averaged. For the biggest TIN-20 experiment, twenty classes are selected randomly as ID and 180 as OOD from the TinyImageNet dataset [38]. For the above experiments we use the same splits as in [5] for compatibility with previous results.

Finally, to test this type of settings to its limits, we evaluate on the fine-grained class splits from the Semantic Shift Benchmark [40]. Here three splits are given: easy, medium and hard, with increasing semantic shift overlap with ID classes. This overlap is determined from a set of detailed

class attributes. We use the splits for the CUB [41] (birds), StanfordCars [17], and FGVC-Aircraft datasets [25].

DS and SS mixed. Another common experimental setting is to consider CIFAR10 as ID and use other datasets as OOD [23, 5, 34, 40]. In this case there is an explicit SS and an implicit DS. We evaluate against MNIST [8], SVHN [26], Textures [7], Places365 [50], CIFAR100 [18], iNaturalist [39], TinyImageNet [38] and LSUN datasets [43].

DS only. Special kind of shift is when the classes stay the same, but the image domain changes. For this experiment we adopt the benchmark from [5] based on DomainNet dataset [30]. The challenge is to distinguish between photos of objects from 173 classes (ID) and clipart/quickdraw images from the same classes (OOD). The benchmark also contains an OOD part with real images from different 173 classes (SS task).

4.2. Evaluation Metrics

There seems to be no consensus, which metrics to report for OOD detection. The most commonly used is the AUROC metric, which measures the ability to distinguish OOD data from ID data. Often this is the only metric reported even though it does not show, how well the method perform on the ID classification task. For ID classification people report either the ID accuracy, FPR95 or OSCR score. In the tables in Sec 4 we report the most commonly used metric for particular OOD problem.

Assuming a binary ID vs OOD classification problem, the **AUROC** measures the area under the true positive (TP) – false positive (FP) rates curve, where the ID data is considered be the positive class. We adopt the evaluation code from [40, 5].

The **FPR at 95% TPR (FPR95)** metric measures the false positive rate at 95% true positive rate on the same binary problem as the AUROC measure.

The Open-Set Classification Rate (**OSCR**) [9, 5] measures the trade-off between the ID classification accuracy and OOD detection accuracy. It is computed as area under CCR(θ)-FPR(θ) curve where CCR(θ) is the correct classification rate defined as

$$\text{CCR}(\theta) = \frac{|\{x \in \mathcal{T}_k | \arg \max_j p(j|x) = k \wedge p(k|x) \geq \theta\}|}{|\mathcal{T}_k|}, \quad (2)$$

where \mathcal{T}_k is the sub-set of the ID training data belonging to the class k , and FPR(θ) is the false positive rate defined as

$$\text{FPR}(\theta) = \frac{|\{x \in \mathcal{U} | \max_k p(k|x) \geq \theta\}|}{|\mathcal{U}|}, \quad (3)$$

where \mathcal{U} is the set of OOD data available at the test time.

Finally, the **ACC** measures the accuracy on the ID classification problem.

arch	pre-trained	classif	SS only		SS + DS	
			AUROC↑	OSCR↑	AUROC↑	FPR95↓
ViT-L/16	ImageNet	LP	91.82	86.92	95.98	21.20
	ImageNet	NM	77.67	69.05	81.48	69.34
ViT-L/14	CLIP	LP	94.35	91.10	97.01	8.73
	CLIP	NM	85.05	79.26	98.06	8.62

Table 1. The CLIP representation consistently outperforms the ImageNet pre-trained representation on a range of OOD tasks. The scores are averages over many semantic-shift-only (SS) and mixed SS and domain shift (SS+DS) tasks. The SS experiments are MNIST, SVHN, CIFAR10, CIFAR+10, CIFAR+50 and TIN, SS+DS experiments include CIFAR10 vs. SVHN, MNIST, Textures, Places365, CIFAR-100, iNaturalist, TIN and LSUN. Evaluation for different network architectures and per-dataset results are provided in the supplementary material.

4.3. Low-Complexity Classifiers

As we argue for a good and general enough representation as the basis for the OOD detection, we use only simple low-complexity classifiers (*i.e.* letting the representation play the essential part in the decision). In particular, we use the Linear Probe (LP) and the Nearest Mean (NM) classifiers. The LP classifier is trained on the ID data only. We use the training code from [31]. As an OOD detection score we use the Maximum logit [40]. The NM classifier’s means are also estimated on the ID data only. The NM similarity is computed from the NM L_2 distance d_{NM} as $1/(1 + d_{NM})$.

4.4. Power of a Good Representation

We start by investigating the effect of different pre-trained representations on various OOD problems. We consider two rich representations: one trained with full supervision on the ImageNet1k classification task and the CLIP representation [31] trained using a self-supervised contrastive objective on a large dataset of image-text description pairs.

The ImageNet pre-trained representation proved to be a strong baseline for many problems in computer vision. We use the ViT-L/16 model pre-trained on ImageNet1k available in the PyTorch Torchvision library and use its penultimate layer as a feature extractor. It produces 1048-dimensional feature vectors.

The CLIP representation has shown outstanding performance on various zero-shot classification problems [31] demonstrating its versatility. From the point of view of OOD detection, what makes the representation appealing is that it was trained on image-text pairs instead of a fixed set of classes. This, together with the self-supervised training possibly allows the model to extract very rich representation of the visual world. This makes it a good candidate for separating ID classes from OOD data irrespective of the type of semantic and distribution shift if these shifts are covered by natural language and represented sufficiently by the training data. The CLIP model (we are using only the image

encoder) produces 768-dimensional feature vectors.

We have also considered smaller ImageNet and CLIP models, but they perform consistently worse, please refer to supplementary materials for smaller models results.

For both representations, we train LP and NM classifiers and test over a range of tasks. We obtain consistent relative performance over different OOD tasks hence we report only the average metrics. We refer to supplementary materials for full results. Table 1 reports the average performance on the studied benchmarks. Our results show that the CLIP representation works better irrespective of the classifier and the type of OOD shift. Hence, we rely on this representation in the following experiments.

4.5. Complementarity of LP and NM

Table 1 shows that the LP and NM classifiers are complementary, each performing well on different types of dataset. It is further illustrated in Figure 1. The plots show LP and NM scores distributions for different ID and OOD datasets.

We observed that for OOD tasks where ID and OOD classes are from the same domain (*e.g.* 6-vs-4 experiment on MNIST) and are thus close to each other in the considered representation, LP tends to work better by finding a suitable linear projection where the ID classes can be well separated whereas the NM classifier struggles distinguishing small distances in the high-dimensional representation (Fig 1a). When the ID and OOD classes are from rather distant domains (*e.g.* CIFAR10 and Places365), the NM method works better as the L_2 distance starts to be discriminative (Fig 1b). And there are some problems (*e.g.* CIFAR10 vs SVHN) where both classifiers produce similarly good separation between ID and OOD classes (Fig 1c).

These observations motivated the development of the combined GROOM method described in Sec 3.

4.6. Mis-calibration of the Logit Scores

Another issue revealed in our experiments is mis-calibration of the maximum logit (or probability) approaches [40, 12, 22, 11]. We demonstrate this in Fig 2. When a logit score threshold is selected (10 in the figure), it produces different false negative rates for each class. This is in contrast with GROOM method, where the threshold is imposed directly on the class false negative (FN) rate. This allows to specify an allowed FN rate while minimizing the FP rate (*i.e.* the number of OOD data classified as ID). This quality is important in safe-critical applications where certain classes are reported as OOD more often or in social-related applications where having uneven FN rates on ID classes may lead to unwanted biases.

4.7. GROOM vs State-of-the-Art

Finally, we compare GROOM with state-of-the-art methods on an extensive range of benchmarks. See the results in

		AUROC \uparrow						Average
	from	MNIST	SVHN	CIFAR10	CIFAR+10	CIFAR+50	TIN	
Deep KNN [34]	[45]	97.50	—	86.90	—	—	74.10	86.17 \dagger
DeepEnsemble [20]	[45]	97.20	—	87.80	—	—	76.00	87.00 \dagger
Pixmix [15]	[45]	93.90	—	90.90	—	—	73.50	86.10 \dagger
OpenHybrid [48]	[40]	99.50	94.70	95.00	96.20	95.50	79.30	93.37
MLS [40]	[40]	99.30	97.10	93.60	97.90	96.50	83.00	94.57
ARPL+CS [5]	[5]	99.70\pm0.10	96.70\pm0.20	91.00 \pm 0.70	97.10 \pm 0.30	95.10 \pm 0.20	78.20 \pm 1.30	92.97 \pm 0.47
LP	ours	97.40 \pm 0.57	78.32 \pm 0.65	98.28\pm0.60	99.32\pm0.38	98.15\pm0.15	94.64\pm0.62	94.35\pm0.50
NM	ours	84.44 \pm 1.28	57.73 \pm 1.69	90.93 \pm 1.31	93.79 \pm 1.40	93.46 \pm 0.55	89.92 \pm 1.53	85.05 \pm 1.29
GROOD	ours	96.88 \pm 0.47	76.14 \pm 1.14	97.76\pm0.43	98.88\pm0.38	98.31\pm0.25	94.18\pm0.94	93.69 \pm 0.60

		OSCR \uparrow						Average
	from	MNIST	SVHN	CIFAR10	CIFAR+10	CIFAR+50	TIN	
ARPL+CS [5]	[5]	99.50 \pm 0.10	94.30 \pm 0.30	87.90 \pm 1.50	94.70 \pm 0.70	92.90 \pm 0.30	65.90 \pm 3.80	89.20 \pm 1.12
LP	ours	96.76 \pm 0.61	65.61 \pm 1.10	97.08 \pm 1.00	98.50 \pm 0.50	97.36 \pm 0.22	91.27 \pm 1.66	91.10 \pm 0.85
NM	ours	76.86 \pm 1.36	41.94 \pm 2.03	88.61 \pm 1.05	92.12 \pm 1.90	91.78 \pm 0.62	84.23 \pm 2.15	79.26 \pm 1.52
GROOD	ours	95.75 \pm 0.58	62.01 \pm 1.41	96.56 \pm 0.60	98.10 \pm 0.51	97.50 \pm 0.16	89.39 \pm 1.79	89.89 \pm 0.84

Table 2. Comparison with the state-of-the-art – OOD problems with semantic shift only. For the description of the measures see Sec 4.2. Averages computed from available results only are marked by \dagger . The OSCR score was reported only by ARPL+CS method.

		FPR at 95% TPR \downarrow / AUROC \uparrow								Average
	from	SVHN	MNIST	Textures	Places365	CIFAR-100	iNaturalist	TIN	LSUN	
Deep KNN [34]	[45]	33.32 / 95.13	50.08 / 91.63	46.01 / 92.77	43.78 / 91.82	52.49 / 89.55	—	46.66 / 91.41	—	45.39 / 92.05 \dagger
	[34]	2.40 / 99.52	—	8.09 / 98.56	23.02 / 95.36	—	—	—	1.78 / 99.48	8.82 / 98.23 \dagger
LogitNorm [42]	[45]	5.30 / 98.86	4.75 / 98.82	30.94 / 94.30	31.17 / 94.76	46.99 / 91.13	—	36.34 / 93.90	—	25.92 / 95.30 \dagger
UDG [44]	[45]	61.91 / 92.50	39.32 / 93.81	43.97 / 93.56	42.44 / 93.58	55.33 / 90.38	—	42.48 / 93.33	—	47.58 / 92.86 \dagger
DeepEnsemble [20]	[45]	37.03 / 94.95	41.65 / 94.34	48.39 / 92.59	50.20 / 91.06	54.31 / 89.76	—	48.93 / 91.35	—	46.75 / 92.34 \dagger
Pixmix [15]	[45]	13.70 / 98.01	49.72 / 91.78	8.07 / 98.83	38.51 / 94.03	47.12 / 91.81	—	36.47 / 94.31	—	32.27 / 94.80 \dagger
ARPL+CS[5]	\ddagger	53.20 / 90.64	42.44 / 94.13	51.84 / 90.68	47.42 / 90.72	57.11 / 88.52	56.02 / 89.73	53.40 / 88.61	46.32 / 91.85	50.97 / 90.61
LP	ours	0.95 / 99.30	0.25 / 99.68	4.11 / 98.46	16.84 / 94.08	10.89 / 97.50	8.29 / 97.73	21.73 / 91.46	6.78 / 97.85	8.73 / 97.01
NM	ours	0.03 / 99.71	0.81 / 98.71	0.00 / 100.00	0.00 / 100.00	65.83 / 86.74	0.00 / 100.00	2.27 / 99.35	0.00 / 100.00	8.62 / 98.06
GROOD	ours	0.00 / 99.97	0.20 / 99.74	0.09 / 99.96	1.05 / 99.78	13.41 / 97.32	0.00 / 100.00	11.11 / 95.97	0.00 / 100.00	3.23 / 99.09

Table 3. Comparison with the state-of-the-art – OOD problems with mixed semantic and domain shifts. The \dagger symbol denotes that the average is computed using available results only. The method marked with \ddagger was trained by us. The measures are described in Sec 4.2.

Tab 2-5. In all the tables we compare against a selection of best performing methods collected from literature and indicate the respective source publication. For comparison with many other methods see the benchmark papers [45, 46, 40].

Tab 2 and Tab 3 summarize the most common benchmarks used in literature, the first one with the semantic shift only and the other with mixed semantic and domain shifts. Once again, the complementarity of LP and NM approaches is clearly visible. The GROOD method performs similarly to the better of the two on individual problems and its performance is consistent over different types of OOD detection tasks; on average it is better. Note that *not outperforming both constituent methods on some particular problems is not a weakness of the method*. In classifier combination, a guarantee of being as good as the better (or best) of a set of classifiers requires an oracle; being outperformed on some particular problem could mean that the simple classifier is overfitted to the problem or its assumptions match the prob-

lem. Compared to state-of-the-art methods, GROOD outperforms all of them by a large margin on most of the OOD problems. Especially on the mixed semantic and domain shift problems in Tab 3, our approach basically solves all the benchmarks.

The proposed method is the most effective on more complex problems like CIFAR variants and TIN and struggles a bit on the 6-vs-4 SVHN problem in Tab 2. We attribute this mainly to the dataset ground truth construction. The images do not contain the single digit stated in GT label but also “some distracting digits to the sides of the digit of interest”³). For CLIP which was trained on many images containing text (with correct label) all digits in the image influence the representation. The performance drop does not happen for MNIST dataset with a single digit per-image, which supports our analysis. Since method that train the representation on ID data does not suffer from this phenom-

³<http://ufldl.stanford.edu/housenumbers>

		ID: Real-A(0 . . . 172) [AUROC ↑ / OSCR ↑]				
	from	Real-B	Clipart-A	Clipart-B	Quickdraw-A	Quickdraw-B
ARPL+CS	[5]	75.20 / 61.90	72.70 / 59.40	82.90 / 66.60	86.70 / 69.00	87.50 / 69.50
LP	ours	93.06 / 87.32	74.00 / 69.43	95.29 / 89.35	96.27 / 90.35	97.38 / 91.11
NM	ours	81.08 / 71.69	68.15 / 60.24	84.77 / 74.91	81.29 / 71.92	82.28 / 72.79
GROOD	ours	91.50 / 83.54	71.84 / 65.20	93.31 / 85.19	89.91 / 81.98	91.11 / 82.83

Table 4. Comparison with the state-of-the-art – OOD problems with a semantic shift (Real-B column) and domain shift only (next four columns). For the description of the measures see Sec 4.2.

		CUB [Easy / Hard]			SCars [Easy / Hard]			FGVC-Aircraft [Easy / Hard]		
	from	ACC	AUROC	OSCR	ACC	AUROC	OSCR	ACC	AUROC	OSCR
ARPL+	[40]	85.90	83.50 / 75.50	76.00 / 69.60	96.90	94.80 / 83.60	92.80 / 82.30	91.50	87.00 / 77.70	83.30 / 74.90
MLS	[40]	86.20	88.30 / 79.30	79.80 / 73.10	97.10	94.00 / 82.20	92.20 / 81.10	91.70	90.70 / 82.30	86.80 / 79.80
LP	ours	93.13	90.38 / 72.74	84.00 / 67.52	97.20	91.15 / 83.85	88.55 / 81.42	73.86	59.42 / 67.07	49.22 / 53.95
NM	ours	90.88	85.07 / 67.16	77.12 / 60.78	94.02	79.63 / 70.52	74.99 / 66.33	66.73	54.56 / 65.79	41.01 / 48.60
GROOD	ours	90.12	91.69 / 72.83	82.49 / 65.38	96.82	89.74 / 85.16	86.79 / 82.31	70.8	78.42 / 54.18	58.40 / 42.62

Table 5. Comparison with the state-of-the-art – OOD problems with fine-grained semantic shift. For the description of the measures see Sec 4.2.

ena, these issues can be potentially alleviated by fine-tuning the representation or using more complex classifiers.

GROOD is also very efficient on the problems with domain shift only as shown in Tab 4. Here our method again outperforms the current state-of-the-art significantly, showing the ability to distinguish data even along such distribution shifts like real-image vs clipart vs quick draw. There is still a space for improvement on the Clipart-A split which is very similar to the ID Real-A dataset (same classes, photos vs complex clipart). This is though difficult even for ARPL+CS which is trained on the ID data.

Finally, to test the limits of the proposed method we evaluated GROOD on the Semantic Shift Benchmark problems with very fine-grained semantic shift in Tab 5. Although the class separation is often very subtle, our method performs comparably to state-of-the-art. The Easy/Hard splits in SCars and FGVC-Aircrafts datasets (in contrast to CUB) are not based on strictly visual attributes, but on attributes like year of production or aircraft variant. They do not seem to correspond to differences captured by the CLIP representation. This is more pronounced in case of airplanes where, e.g., the overall shape do not change between production years (as oppose to cars). We see this as a border case and a weakness of the benchmark⁴ and a possible future direction.

Overall, the experiments demonstrate how using a powerful representation leads not only to a state-of-the-art ID classification as demonstrated earlier [31], but provides classifier with very strong cues for OOD detection as well.

⁴“...open-set bins of different difficulties in Stanford Cars are the most troublesome to define. This is because the rough hierarchy in the class names may not always correspond to the degree of visual similarity between the classes”[40].

5. Conclusions

In this paper we propose a novel approach to OOD detection which uses a generic pre-trained representation instead of training a discriminative classifier on the ID classes. In initial experiments, two low-complexity classifiers already significantly outperform other state-of-the-art methods on most considered OOD benchmarks, confirming the applicability of the used representation for the OOD detection.

As a second novelty, we model the classification scores of the two classifiers for the ID classes as a multivariate Gaussian and show that this permits addressing OOD detection as a formally defined two-class Neyman-Pearson task. Compared to traditional logit thresholding, the solution to this task leads to naturally calibrated OOD detection score connected directly to the same false negative rate on all ID classes. Moreover, the resulting GROOD method leverages the strengths of both used classifiers leading to consistent and superior performance over all considered benchmarks.

The proposed GROOD method was compared to the state-of-the-art methods on a very wide range of OOD problems with diverse types and strengths of semantic and domain shifts. It effectively solves the mixed semantic and distribution shift benchmarks and achieves the best performance on most of the other considered problems.

The only observed limitations are related to very small low-contrast images in SVHN dataset and very fine-grained classification of airplanes, which we hypothesise requires a more complex use of the ID training data.

The simplicity of the adaptation of the GROOD method to a novel problem – only a multi-class logistic regression, i.e. a linear layer followed by a softmax, is needed for training – make the process fast.

We suggest that the proposed method combined with a generic representation is suitable for most OOD tasks based on natural images and it remains open for the research community to show any possible failure cases in new benchmarks; with GOOD many of the standard benchmarks are saturated and no longer stimulate further progress.

Acknowledgement This work was supported by Toyota Motor Europe. We would also like to thank Jonáš Šerých for many valuable discussions related to this paper.

References

- [1] Paul Bergmann, Kilian Batzner, Michael Fauser, David Sattlegger, and Carsten Steger. The MVTec Anomaly Detection Dataset: A Comprehensive Real-World Dataset for Unsupervised Anomaly Detection. *IJCV*, 129(4):1038–1059, 2021.
- [2] Julian Bitterwolf, Alexander Meinke, Maximilian Augustin, and Matthias Hein. Breaking down out-of-distribution detection: Many methods based on ood training data estimate a combination of the same core quantities, 2022.
- [3] Daniel Bogdoll, Maximilian Nitsche, and J. Marius Zollner. Anomaly detection in autonomous driving: A survey. In *2022 IEEE/CVF Conference on Computer Vision and Pattern Recognition Workshops (CVPRW)*. IEEE, jun 2022.
- [4] Robin Chan, Krzysztof Lis, Svenja Uhlemeyer, Hermann Blum, Sina Honari, Roland Siegwart, Pascal Fua, Mathieu Salzmann, and Matthias Rottmann. SegmentMeIfYouCan: A Benchmark for Anomaly Segmentation, 2021.
- [5] Guangyao Chen, Peixi Peng, Xiangqian Wang, and Yonghong Tian. Adversarial reciprocal points learning for open set recognition. *IEEE Transactions on Pattern Analysis and Machine Intelligence*, 2021.
- [6] Ting Chen, Simon Kornblith, Mohammad Norouzi, and Geoffrey Hinton. A simple framework for contrastive learning of visual representations. In *International conference on machine learning*, pages 1597–1607. PMLR, 2020.
- [7] Mircea Cimpoi, Subhansu Maji, Iasonas Kokkinos, Sammy Mohamed, and Andrea Vedaldi. Describing textures in the wild. In *Proceedings of the IEEE conference on computer vision and pattern recognition*, pages 3606–3613, 2014.
- [8] Li Deng. The mnist database of handwritten digit images for machine learning research. *IEEE signal processing magazine*, 29(6):141–142, 2012.
- [9] Akshay Raj Dhamija, Manuel Günther, and Terrance E. Boult. Reducing network agnostophobia. In *NeurIPS*, 2018.
- [10] Dan Hendrycks, Steven Basart, Mantas Mazeika, Mohammadreza Mostajabi, Jacob Steinhardt, and Dawn Song. Scaling out-of-distribution detection for real-world settings. *ICML*, 2022.
- [11] Dan Hendrycks, Steven Basart, Mantas Mazeika, Andy Zou, Joe Kwon, Mohammadreza Mostajabi, Jacob Steinhardt, and Dawn Song. Scaling out-of-distribution detection for real-world settings. *ICML*, 2022.
- [12] Dan Hendrycks and Kevin Gimpel. A baseline for detecting misclassified and out-of-distribution examples in neural networks. *arXiv preprint arXiv:1610.02136*, 2016.
- [13] Dan Hendrycks, Kimin Lee, and Mantas Mazeika. Using pre-training can improve model robustness and uncertainty. In *International Conference on Machine Learning*, pages 2712–2721. PMLR, 2019.
- [14] Dan Hendrycks, Mantas Mazeika, Saurav Kadavath, and Dawn Song. Using self-supervised learning can improve model robustness and uncertainty. *Advances in neural information processing systems*, 32, 2019.
- [15] Dan Hendrycks, Andy Zou, Mantas Mazeika, Leonard Tang, Bo Li, Dawn Song, and Jacob Steinhardt. Pixmix: Dream-like pictures comprehensively improve safety measures. In *Proceedings of the IEEE/CVF Conference on Computer Vision and Pattern Recognition*, pages 16783–16792, 2022.
- [16] Yen-Chang Hsu, Yilin Shen, Hongxia Jin, and Zsolt Kira. Generalized odin: Detecting out-of-distribution image without learning from out-of-distribution data. In *Proceedings of the IEEE/CVF Conference on Computer Vision and Pattern Recognition*, pages 10951–10960, 2020.
- [17] Jonathan Krause, Michael Stark, Jia Deng, and Li Fei-Fei. 3d object representations for fine-grained categorization. In *Proceedings of the IEEE international conference on computer vision workshops*, pages 554–561, 2013.
- [18] Alex Krizhevsky. Learning multiple layers of features from tiny images. Technical report, 2009.
- [19] Weicheng Kuo, Christian Häne, Pratik Mukherjee, Jitendra Malik, and Esther Yuh. Expert-level detection of acute intracranial hemorrhage on head computed tomography using deep learning. *Proceedings of the National Academy of Sciences*, 116:201908021, 10 2019.
- [20] Balaji Lakshminarayanan, Alexander Pritzel, and Charles Blundell. Simple and scalable predictive uncertainty estimation using deep ensembles. *Advances in neural information processing systems*, 30, 2017.
- [21] Kimin Lee, Kibok Lee, Honglak Lee, and Jinwoo Shin. A simple unified framework for detecting out-of-distribution samples and adversarial attacks. In *Advances in Neural Information Processing Systems*, pages 7167–7177, 2018.
- [22] Shiyu Liang, Yixuan Li, and Rayadurgam Srikant. Enhancing the reliability of out-of-distribution image detection in neural networks. *arXiv preprint arXiv:1706.02690*, 2017.
- [23] Weitang Liu, Xiaoyun Wang, John Owens, and Yixuan Li. Energy-based out-of-distribution detection. *Advances in Neural Information Processing Systems*, 33:21464–21475, 2020.
- [24] Atefeh Mahdavi and Marco Carvalho. A survey on open set recognition. In *2021 IEEE Fourth International Conference on Artificial Intelligence and Knowledge Engineering (AIKE)*. IEEE, dec 2021.
- [25] Subhansu Maji, Esa Rahtu, Juho Kannala, Matthew Blaschko, and Andrea Vedaldi. Fine-grained visual classification of aircraft. *arXiv preprint arXiv:1306.5151*, 2013.
- [26] Yuval Netzer, Tao Wang, Adam Coates, A. Bissacco, Bo Wu, and A. Ng. Reading digits in natural images with unsupervised feature learning. In *NIPS Workshop on Deep Learning and Unsupervised Feature Learning*, 2011.
- [27] Jerzy Neyman and Egon S Pearson. On the use and interpretation of certain test criteria for purposes of statistical inference. *Biometrika*, pages 175–240, 1928.

- [28] Jerzy Neyman and Egon Sharpe Pearson. Ix. on the problem of the most efficient tests of statistical hypotheses. *Philosophical Transactions of the Royal Society of London. Series A, Containing Papers of a Mathematical or Physical Character*, 231(694-706):289–337, 1933.
- [29] Oleksiy Ostapenko, Timothee Lesort, Pau Rodríguez, Md Rifat Arefin, Arthur Douillard, Irina Rish, and Laurent Charlin. Continual learning with foundation models: An empirical study of latent replay. In *Conference on Lifelong Learning Agents*, pages 60–91. PMLR, 2022.
- [30] Xingchao Peng, Qinxun Bai, Xide Xia, Zijun Huang, Kate Saenko, and Bo Wang. Moment matching for multi-source domain adaptation. In *Proceedings of the IEEE/CVF international conference on computer vision*, pages 1406–1415, 2019.
- [31] Alec Radford, Jong Wook Kim, Chris Hallacy, Aditya Ramesh, Gabriel Goh, Sandhini Agarwal, Girish Sastry, Amanda Askell, Pamela Mishkin, Jack Clark, et al. Learning transferable visual models from natural language supervision. In *International Conference on Machine Learning*, pages 8748–8763. PMLR, 2021.
- [32] Michail I. Schlesinger and Vaclav Hlavac. *Ten Lectures on Statistical and Structural Pattern Recognition*. Computational Imaging and Vision, 2002.
- [33] Yiyu Sun, Chuan Guo, and Yixuan Li. React: Out-of-distribution detection with rectified activations. *Advances in Neural Information Processing Systems*, 34:144–157, 2021.
- [34] Yiyu Sun, Yifei Ming, Xiaojin Zhu, and Yixuan Li. Out-of-distribution detection with deep nearest neighbors. *ICML*, 2022.
- [35] Jihoon Tack, Sangwoo Mo, Jongheon Jeong, and Jinwoo Shin. Csi: Novelty detection via contrastive learning on distributionally shifted instances. *Advances in neural information processing systems*, 33:11839–11852, 2020.
- [36] Sunil Thulasidasan, Gopinath Chennupati, Jeff A Bilmes, Tanmoy Bhattacharya, and Sarah Michalak. On mixup training: Improved calibration and predictive uncertainty for deep neural networks. *Advances in Neural Information Processing Systems*, 32, 2019.
- [37] Yonglong Tian, Yue Wang, Dilip Krishnan, Joshua B Tenenbaum, and Phillip Isola. Rethinking few-shot image classification: a good embedding is all you need? In *Computer Vision–ECCV 2020: 16th European Conference, Glasgow, UK, August 23–28, 2020, Proceedings, Part XIV 16*, pages 266–282. Springer, 2020.
- [38] Antonio Torralba, Rob Fergus, and William T Freeman. 80 million tiny images: A large data set for nonparametric object and scene recognition. *IEEE transactions on pattern analysis and machine intelligence*, 30(11):1958–1970, 2008.
- [39] Grant Van Horn, Oisin Mac Aodha, Yang Song, Yin Cui, Chen Sun, Alex Shepard, Hartwig Adam, Pietro Perona, and Serge Belongie. The inaturalist species classification and detection dataset. In *Proceedings of the IEEE conference on computer vision and pattern recognition*, pages 8769–8778, 2018.
- [40] Sagar Vaze, Kai Han, Andrea Vedaldi, and Andrew Zisserman. Open-set recognition: A good closed-set classifier is all you need. In *International Conference on Learning Representations*, 2022.
- [41] Catherine Wah, Steve Branson, Peter Welinder, Pietro Perona, and Serge Belongie. The caltechucsd birds-200-2011 dataset. Technical Report CNS-TR-2011-001, California Institute of Technology, 2011.
- [42] Hongxin Wei, Renchunzi Xie, Hao Cheng, Lei Feng, Bo An, and Yixuan Li. Mitigating neural network overconfidence with logit normalization. *ICML*, 2022.
- [43] Jianxiong Xiao, James Hays, Krista A Ehinger, Aude Oliva, and Antonio Torralba. Sun database: Large-scale scene recognition from abbey to zoo. In *2010 IEEE computer society conference on computer vision and pattern recognition*, pages 3485–3492. IEEE, 2010.
- [44] Jingkang Yang, Haoqi Wang, Litong Feng, Xiaopeng Yan, Huabin Zheng, Wayne Zhang, and Ziwei Liu. Semantically coherent out-of-distribution detection. *2021 IEEE/CVF International Conference on Computer Vision (ICCV)*, pages 8281–8289, 2021.
- [45] Jingkang Yang, Pengyun Wang, Dejian Zou, Zitang Zhou, Kunyuan Ding, Wenxuan Peng, Haoqi Wang, Guangyao Chen, Bo Li, Yiyu Sun, et al. OpenOOD: Benchmarking generalized out-of-distribution detection. In *Thirty-sixth Conference on Neural Information Processing Systems Datasets and Benchmarks Track*, 2022.
- [46] Jingkang Yang, Kaiyang Zhou, Yixuan Li, and Ziwei Liu. Generalized out-of-distribution detection: A survey. *arXiv preprint arXiv:2110.11334*, 2021.
- [47] Sangdoo Yun, Dongyoon Han, Seong Joon Oh, Sanghyuk Chun, Junsuk Choe, and Youngjoon Yoo. Cutmix: Regularization strategy to train strong classifiers with localizable features. In *Proceedings of the IEEE/CVF international conference on computer vision*, pages 6023–6032, 2019.
- [48] Hongjie Zhang, Ang Li, Jie Guo, and Yanwen Guo. Hybrid models for open set recognition. In *ECCV*, 2020.
- [49] Zhilin Zhao, Longbing Cao, and Kun-Yu Lin. Revealing distributional vulnerability of explicit discriminators by implicit generators. *CoRR*, abs/2108.09976, 2021.
- [50] Bolei Zhou, Agata Lapedriza, Aditya Khosla, Aude Oliva, and Antonio Torralba. Places: A 10 million image database for scene recognition. *IEEE transactions on pattern analysis and machine intelligence*, 40(6):1452–1464, 2017.